Measurements of secondary electron emission effects in the Hall thruster discharge

Y. Raitses, A. Smirnov, D. Staack, and N. J. Fisch
Princeton Plasma Physics Laboratory, Princeton, New Jersey 08543

(Received 24 October 2005; accepted 8 December 2005; published online 12 January 2006)

The dependence of the maximum electron temperature on the discharge voltage is studied for two Hall thruster configurations, in which a collisionless plasma is bounded by channel walls made of materials with different secondary electron emission (SEE) properties. The linear growth of the temperature with the discharge voltage, observed in the channel with a low SEE yield, suggests that SEE is responsible for the electron temperature saturation in the thruster configuration with the channel walls having a higher SEE yield. The fact that the values of the electron temperature at saturation are rather high may indirectly support the recently predicted kinetic regime of the space charge saturation of the near-wall sheath in the thruster discharge. A correlation between the effects of the channel wall material on the electron temperature and the electron cross-field current was also observed. © *2006 American Institute of Physics*. [DOI: 10.1063/1.2162809]

Secondary electron emission (SEE) from the wall bounding a plasma reduces the sheath potential drop and, thereby, weakens thermal insulating properties of the sheath.[1] In a quasineutral plasma, the flux of secondary electrons into the plasma cannot increase above the value that corresponds to the space charge saturated (SCS) sheath. At this critical point the fluxes of secondary electrons from the wall and primary electrons from the plasma are approximately equal, and the wall acts as an extremely effective electron energy sink. The SCS sheath has been the subject of many studies due to its relevance to plasma applications such as, for example, fusion devices,[2] emissive walls,[3] dusty plasmas,[4] and Hall thrusters[5–12] (so-called stationary plasma thrusters or SPTs).

In a SPT,[13,14] the plasma discharge with magnetized electrons and unmagnetized ions is generated in the axial electric and radial magnetic fields applied in an annular ceramic channel. The discharge voltage controls the Joule heating of the electrons, which diffuse across the magnetic field. There is no consensus between the existing fluid and kinetic models on how strong the SEE effects on the thruster plasma are. The fluid models[5,6] predict that SEE is strong enough to enhance electron energy losses at the walls and, thereby, to limit the maximum attainable electron temperature in the thruster channel. According to the kinetic simulations,[7,15–17] the electron energy distribution function (EDF) in a collisionless thruster plasma is depleted at high energy due to electron-wall collisions. Under such conditions, the effects of SEE on the plasma can be substantially weaker.

In recent papers,[11] it was shown experimentally that the maximum attainable electron temperature in the thruster channel is limited, but this limit greatly exceeds the theoretical value obtained for the SCS sheath regime under the assumption of the Maxwellian electron energy distribution function (EDF). This Brief Communication demonstrates how the maximum electron temperature depends on SEE properties of the channel wall material. Although the effects of the wall material on the thruster discharge are well documented in the literature,[5,10,18,19] this work presents new experimental results that show how SEE affects the electron temperature in the thruster plasma.

The thruster, facility, and diagnostics used in these experiments are described elsewhere.[11,20,21] The 2 kW laboratory Hall thruster[11] was operated with two different channels. One channel was made entirely of boron nitride (grade HP), which is a ceramic material with high SEE yield.[16] The other channel had its exit part (where, for SPTs, the electron temperature usually has a local maximum[11,22]) made of carbon, while the rest of the channel was made of boron nitride. For a flat carbon, the SEE yield approaches unity at an order of magnitude higher energy of primary electrons than that for boron nitride.[5] In the described experiments two segmented electrodes[19,23] made of low-sputtering carbon velvet material[21] were placed on the inner and outer channel walls. The lengths of the inner and outer electrodes are 4 and 6 mm, respectively (Fig. 1). Field emission from carbon fibers of the segmented electrodes was shown to have a minor effect on the operation of the segmented thruster.[21]

The experiments took place in a 28 m^3 vacuum vessel equipped with cryogenic pumps. In each configuration, the thruster was operated at a constant xenon mass flow rate of about 2 mg/s. The background pressure did not exceed 6 μTorr. A commercial hollow cathode-neutralizer was operated in a self-sustained mode due to the thruster discharge. The magnetic field (Fig. 1) was held constant. During the operation of the segmented thruster, the electrodes were floating. The electron temperature was deduced from the hot (emissive) and cold probe measurements as described in recent papers.[11,20] The total ion flux from the thruster was measured with a guarding sleeve planar probe.[11,23]

A detailed analysis of the thruster *V-I* characteristics is given in Ref. 21. It was found that the effect of the channel wall material on the discharge current is stronger than that on the ion flux from the thruster (Fig. 2). The current utilization, which is the ratio of the ion current to the discharge current, I_{ion}/I_d, characterizes how effectively the magnetic field im-

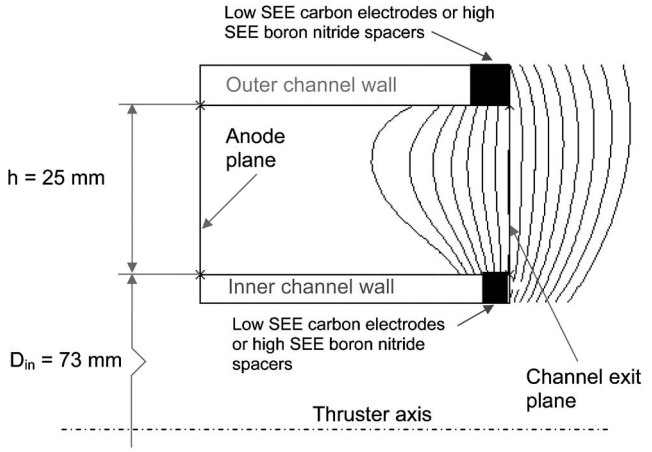

FIG. 1. Schematic of the segmented Hall thruster channel with superimposed magnetic field lines. The magnetic field distribution was simulated for the experimental conditions.

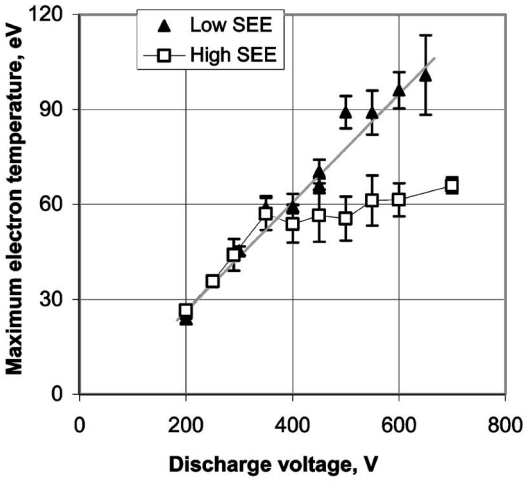

FIG. 3. The dependence of the maximum electron temperature on the discharge voltage for the conventional thruster with high-SEE boron nitride channel walls and the segmented thruster with low-SEE floating segmented electrodes made of carbon velvet material. Reproducibility of measurements is shown by error bars.

pedes the electron cross-field transport.[16] Figure 2 shows that for the conventional thruster, as opposed to the segmented thruster, the impedance degrades with the discharge voltage. The shortening of the plasma electric field through the conductive wall is predicted to increase the discharge current in the segmented thruster, as compared with the conventional thruster.[5,19] The fact that this effect is not so evident from our experiments is, probably, due to the relatively small surface area of the segmented electrodes.[19] There is a certain correlation between the effects of the wall material on the discharge current and on the maximum electron temperature (Fig. 3). Within the accuracy of the probe measurements, the wall material has almost no effect on the maximum electron temperature below the discharge voltage of 400 V. In keeping with the previous experimental observations,[24] this result demonstrates a minor role of the wall material properties for the thruster operation at low to moderate discharge voltage. When the discharge voltage increases above 400 V, the maximum electron temperature saturates in the conventional thruster, but continues to grow in the segmented thruster. Because the key difference between the thruster configurations is in the SEE properties of the channel wall material, it is apparently the SEE that is responsible for the temperature saturation and the electron conductivity enhancement, observed in the conventional thruster with the boron nitride channel walls.

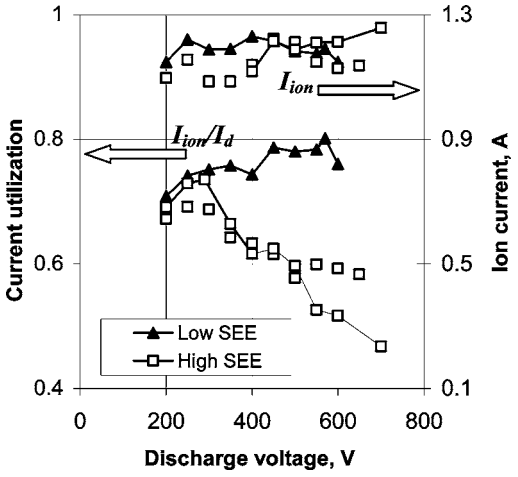

FIG. 2. The current utilization, I_{ion}/I_d and the total ion current, I_{ion}, from the thruster for xenon mass flow rate of about 2 mg/s and a constant magnetic field. Measurements were done for the conventional thruster with high-SEE boron nitride channel walls and the segmented thruster with low-SEE floating segmented electrodes made of carbon velvet material.

Barral *et al.*[5] predicted a qualitatively similar correlation between the discharge current and the maximum electron temperature. According to the fluid model,[5] when the near-wall sheaths become space charge saturated, SEE-enhanced electron-wall collisions lead to an increase of the electron energy loss at the walls and, also, contribute significantly to the electron cross-field transport (near-wall conductivity). However, there is a large quantitative disagreement between the predictions of the fluid models[5,6] and the experimental results[11] with respect to the occurrence of the SCS sheath regime in the thruster plasma. Without going into details of this disagreement,[11] we refer to a recent kinetic study of Sydorenko *et al.*,[7] which demonstrates the existence of the kinetic regime of the SCS sheath in the collisionless thruster plasma with non-Maxwellian electrons. According to the particle-in-cell (PIC) simulations,[7] the electron EDF in the thruster discharge is not only depleted at high energy, but is also strongly anisotropic ($\langle \varepsilon_{e\perp} \rangle / \langle \varepsilon_{e\parallel} \rangle \sim 4$). Thus, the electron temperature parallel to the magnetic field (normal to the walls) can be much smaller than the experimental value deduced from the averaged probe measurements. However, this level of electron energy anisotropy, which was also obtained in the fluid simulations,[5] is still not enough to quantitatively explain high values of the electron temperature at saturation, which are observed in the experiments.[11] The most recent kinetic[7,8] and fluid[9] theories predict, and PIC simulations demonstrate,[7] that cold (2–3 eV) secondary electrons emitted from the two opposite walls of the annular channel and accelerated in the near wall sheaths (to energies of the order

of a few T_e, where $T_e \sim 30-60$ eV) can form counterstreaming beams. When the beam electrons penetrate through the plasma bulk, they gain additional energy (due to $E \times B$ motion), which may be sufficient to induce SEE from the wall.[7] In this case, the total flux of secondary electrons from the wall is $\Gamma_{\mathrm{SEE}} = \gamma_b \Gamma_b + \gamma_p \Gamma_p$, where γ_b and γ_p are the partial SEE coefficients for the beam and bulk plasma electrons, and Γ_b and Γ_p are the corresponding electron fluxes toward the wall. The effective total SEE coefficient $\langle \gamma \rangle \equiv \Gamma_{\mathrm{SEE}}/(\Gamma_b + \Gamma_p)$ can be then expressed as[7,8]

$$\langle \gamma \rangle = \frac{\gamma_p}{1 + \alpha(\gamma_p - \gamma_b)}. \tag{1}$$

Here, $\alpha \equiv \Gamma_b/\Gamma_{\mathrm{SEE}} < 1$ characterizes penetration of the electron beam through the plasma bulk. Under such conditions the sheath becomes space charge saturated when the effective coefficient $\langle \gamma \rangle$ approaches unity. It means that (i) for $\langle \gamma \rangle < 1$, the SEE coefficient due to the plasma bulk electrons, γ_p, is no longer restricted to be less than unity and (ii) the average energy of the plasma bulk electrons can be larger than the critical value that corresponds to the SCS sheath regime in the plasma without the beams.[7,8] Note that using a macroscopic model, Ahedo *et al.*[9] obtained a similar conclusion with respect to $\gamma_p > 1$. However, the model[9] assumes Maxwellian plasma electrons and does not consider the SEE due to the beam electrons, i.e., in Ref. 9, $\gamma_b = 0$. According to Ref. 7, a contribution of the beam electrons to the SEE is critical to plasma-wall interaction in Hall thrusters. It is important to emphasize that although a strong temperature anisotropy and beams of secondary electrons might explain the measured temperature saturation by the kinetic SCS sheath regime, these predictions certainly need an experimental verification.

Note that even though the electron temperature in the segmented thruster grows with the discharge voltage, the total ion flux does not change much and remains almost equal to that in the conventional thruster configuration (see Figs. 2 and 3). This is most likely due to the fact that ionization of neutrals at the interface of the ionization and acceleration regions is compensated by the ion wall losses.[25] The growth of the electron temperature, which tends to enhance ionization, leads also (through quasineutrality) to the increase of the ion wall losses. The fraction of multicharged xenon ions in the ion flux should not be large, because the residence time of Xe^{+1} ions in the acceleration region is much smaller than the time of ionization to higher charge states. For example, for the electron temperature $T_e \sim 100$ eV and plasma density $N_e \sim 5 \times 10^{11}$ cm^{-3}, the rate coefficient for single-electron impact ionization $Xe^{+1} \rightarrow Xe^{+2}$ is about $k \sim 1.2 \times 10^{-7}$ cm^3/s.[26] (When the electron temperature is increased from 50 to 100 eV, the ionization rate grows by about 30% only.) The time of flight of an ion through the acceleration region with length $L \sim 1.5$ cm and voltage drop of about 400 V is $\tau \sim 1$ μs, while the ionization time $\tau_{1,2} \sim (N_e k)^{-1} \sim 16$ μs. Thus, in this regime, we expect the number of ionization events to scale linearly with the residence time. The difference in the fraction of multicharged ions in the conventional and segmented configurations is believed to be small.

In summary, we demonstrated the effect of SEE properties of the channel wall material on the maximum electron temperature and the electron cross-field current. In the thruster with the segmented electrodes that have low SEE yield, the electron temperature increases almost linearly with the discharge voltage. In contrast to that, in the conventional thruster with the boron nitride ceramic channel the electron temperature saturates at high discharge voltage. The recently predicted kinetic regime[7] of the SCS sheath may explain why the electron temperature is observed to saturate at the substantially larger values than those obtained theoretically for the Maxwellian electron EDF. Below the discharge voltage of 400 V, there are no significant differences in the plasma properties (electron temperature and discharge current) for the conventional and segmented thrusters. This result provides evidence of a minor SEE role in the thruster operation below the temperature saturation. Finally, the plasma measurements in the segmented thruster may be relevant to the anode layer Hall thrusters,[27] whose interior plasma properties were predicted[14,28] but, to the best of our knowledge, not measured.

ACKNOWLEDGMENTS

The authors wish to thank Dmytro Sydorenko, Dr. Igor Kaganovich, Dr. Leonid Dorf, and Professor Amnon Fruchtman for useful discussions on this paper.

This work was supported by US DOE Contract No. AC02-76CH0-3073.

[1] G. D. Hobbs and J. A. Wesson, Plasma Phys. **9**, 85 (1967).
[2] P. C. Stangeby, in *The Plasma Boundary of Magnetic Fusion Devices*, Plasma Physics Series (IOP, Bristol, 2000), pp. 646–654.
[3] T. Intrator, M. H. Cho, E. Y. Wang, N. Hershkowitz, D. Diebold, and J. DeKock, J. Appl. Phys. **64**, 2927 (1988); L. A. Schwager, Phys. Fluids B **5**, 631 (1993).
[4] G. L. Delzanno, G. Lapenta, and M. Rosenberg, Phys. Rev. Lett. **92**, 035002 (2004).
[5] S. Barral, K. Makowski, Z. Peradzynski, N. Gascon, and M. Dudeck, Phys. Plasmas **10**, 4137 (2003); N. Gascon, M. Dudeck, and S. Barral, *ibid.* **10**, 4123 (2003).
[6] E. Ahedo, J. M. Gallardo, and M. Martinez-Sanchez, Phys. Plasmas **10**, 3397 (2003).
[7] D. Sydorenko, V. Smolyakov, I. Kaganovich, and Y. Raitses, Phys. Plasmas 13, (2005).
[8] I. Kaganovich, Proceedings of the 29th International Electric Propulsion Conference (Electric Rocket Propulsion Society, Cleveland, OH, 2005), IEPC paper 2005–096.
[9] E. Ahedo and D. I. Parra, Phys. Plasmas **12**, 073503 (2005).
[10] M. Keidar, I. Boyd, and I. I. Beilis, Phys. Plasmas **8**, 5315 (2001).
[11] Y. Raitses, D. Staack, A. Smirnov, and N. J. Fisch, Phys. Plasmas **12**, 073507 (2005); Y. Raitses, D. Staack, M. Keidar, and N. J. Fisch, *ibid.* **12**, 057104 (2005).
[12] F. Taccogna, S. Longo, and M. Capitelli, Phys. Plasmas **12**, 093506 (2005).
[13] A. I. Morozov and V. V. Savel'ev, in *Reviews of Plasma Physics*, edited by B. B. Kadomtsev and V. D. Shafranov (Consultants Bureau, New York, 2000), Vol. 21.
[14] E. Y. Choueiri, Phys. Plasmas **8**, 5025 (2001).
[15] N. Meeazan and M. Cappelli, Phys. Rev. E **66**, 036401 (2002).
[16] A. Smirnov, Y. Raitses, and N. J. Fisch, Phys. Plasmas **11**, 4922 (2004).
[17] O. Batishchev and M. Martinez-Sanchez, Proceedings of the 28th International Electric Propulsion Conference, March 2003, Toulouse, France (Electric Rocket Propulsion Society, Cleveland, OH, 2003), IEPC paper 2003–188.

[18]J. Ashkenazy, Y. Raitses, and G. Appelbaum, Phys. Plasmas **5**, 2055 (1998).
[19]Y. Raitses M. Keidar, D. Staack, and N. J. Fisch, J. Appl. Phys. **92**, 4906 (2002); D. Staack, Y. Raitses, and N. J. Fisch, Proceedings of the 28th International Electric Propulsion Conference (Electric Rocket Propulsion Society, Cleveland, OH, 2003), IEPC paper 2003–157.
[20]D. Staack, Y. Raitses, and N. J. Fisch, Rev. Sci. Instrum. **75**, 393 (2004); A. Smirnov, Y. Raitses, and N. J. Fisch, J. Appl. Phys. **94**, 852 (2003).
[21]Y. Raitses, D. Staack, and N. J. Fisch, to appear in J. Appl. Phys.
[22]J. M. Haas and A. D. Gallimore, Phys. Plasmas **8**, 652 (2001).
[23]A. Fruchtman, N. J. Fisch, and Y. Raitses, Phys. Plasmas **8**, 1048 (2001); Y. Raitses, L. A. Dorf, A. A. Litvak, and N. J. Fisch, J. Appl. Phys. **88**, 1263 (2000); N. J. Fisch, Y. Raitses, L. A. Dorf, and A. A. Litvak, *ibid.* **89**, 2040 (2001).
[24]D. Staack, Y. Raitses, and N. J. Fisch, Appl. Phys. Lett. **84**, 3028 (2004).
[25]L. Dorf, V. Semenov, and Y. Raitses, Appl. Phys. Lett. **83**, 2551 (2003); E. Ahedo and D. Escobar, J. Appl. Phys. **96**, 983 (2004).
[26]E. W. Bell, N. Djuric, and G. H. Dunn, Phys. Rev. A **48**, 4286 (1993).
[27]V. Zhurin, H. Kaufman, and R. Robinson, Plasma Sources Sci. Technol. **8**, R1 (1999).
[28]M. Keidar, I. D. Boyd, and I. Beilis, Phys. Plasmas **11**, 1715 (2004).